CHEMICAL ENGINEERING TRANSACTIONS
VOL. 69, 2018
A publication of AIDIC
The Italian Association of Chemical Engineering
Online at www.aidic.it/cet
Guest Editors: Elisabetta Brunazzi, Eva Sorensen

ISBN 978-88-95608-66-2; **ISSN** 2283-9216

Zero-Gravity Distillation with Metal Foams: A Modelling Approach

Sebastian Rieks[a], Niklas Preußer[b], Tatiana Gambaryan-Roisman[b], Eugeny Y. Kenig[a,*]

[a]Chair of Fluid Process Engineering, Paderborn University, Pohlweg 55, 33098 Paderborn, Germany
[b]Institute for Technical Thermodynamics, TU Darmstadt, Alarich-Weiss-Straße 10, 64287 Darmstadt, Germany
eugeny.kenig@upb.de

Zero-gravity distillation (ZGD) is one of the few ways to establish a small-scale distillation process. In contrast to conventional distillation columns, capillary forces, e.g. induced by metal foams, are exploited to ensure liquid flow in ZGD units. In order to strengthen the knowledge basis necessary for the ZGD equipment design, understanding of the relevant transport phenomena is necessary. In this work, a model for phenomena governing the ZGD processes was developed. It includes momentum, heat and species transport in both liquid and vapour phases. Evaporation and condensation impacts on momentum transfer are captured in a simplified manner, allowing an approximate local flow velocity determination. The developed model was implemented in the OpenFOAM® software and used to numerically simulate methanol/ethanol distillation processes in 2D approximation. In a first numerical study, the influence of the metal foam porosity and thickness on the velocity, temperature and mass fraction fields was numerically investigated.

1. Introduction

To realise the process engineers' vision of an entire suitcase-sized chemical production process, the development of effective small-scale separation units is necessary. This is particularly true for distillation, since this unit operation represents one of the most important separation methods for homogeneous liquid mixtures. Up to now, small-scale distillation units, although being an object of intense research, have not been developed far enough to be applied in production processes. One of the main reasons is that relevant design fundamentals are still missing (Kenig et al., 2013).

Among the few ideas towards small-scale distillation equipment, *zero-gravity distillation* (ZGD) should be named. The first study was published by Seok and Hwang (1985), who investigated ethanol/water and methanol/water separations. Their distillation column consisted of a glass pipe with 10.5 mm diameter and 340 mm length. Fiberglass was used as porous material within the pipe. The column was mounted horizontally so that gravity influences could be avoided. Due to heating and cooling of the opposite column ends, a counter-current flow was established. Seok and Hwang (1985) performed experiments with and without total reflux. A separation efficiency of about 4.5 theoretical stages was reached. They complemented their work with an analytical model of the relevant transport processes during ZGD, based on Darcy's law. For species transfer, a model using experimentally determined mass transfer coefficients was applied.

Despite the great potential of ZGD, only two further groups were engaged in the modelling of this process. Ramirez-Gonzalez et al. (1992) presented an approach based on the Young-Laplace equation and Darcy's law for fluid flow. Here, again, experimentally determined mass transfer coefficients were used for species transfer description. They noticed that the quality of their simulation results was strongly dependent on the correlations used for the mass transfer coefficients. They further reported best results for correlations valid for turbulent flow. This appears questionable, because the flow in such small-scale devices should rather be laminar. Later, Tschernjaew et al. (1996) proposed an alternative approach. Momentum transfer was described similar to Ramirez-Gonzalez et al. (1992), yet species transfer was captured using the Maxwell-Stefan approach for multicomponent mixtures. This species transfer description is independent from experimental data. Tschernjaew et al. (1996) theoretically determined separation efficiencies for the system

ethanol/isopropanol/water. However, their results were not confirmed experimentally. All three modelling methods presented above do not take phase change phenomena into account, and thus, no rigorous model for the simulation of ZGD processes including phase change effects is available. In the present work, such a model is proposed for ZGD with metal foam structures.

2. Mathematical model

In this section, a model for coupled momentum, heat and species transport within a ZGD apparatus is presented. The apparatus is filled with a two-phase binary system. Liquid is embedded in a porous structure (metal foam) and covered by a vapour phase. The bottom of the porous structure is heated at the evaporator zone and cooled at the condenser zone. Via the liquid inlet and vapour outlet, it is connected to a separate reservoir, which contains both liquid and vapour phase. In the present work, the transport phenomena within the unit are modelled in two-dimensional approximation. The corresponding computational domain with its boundary conditions is depicted in Figure 1.

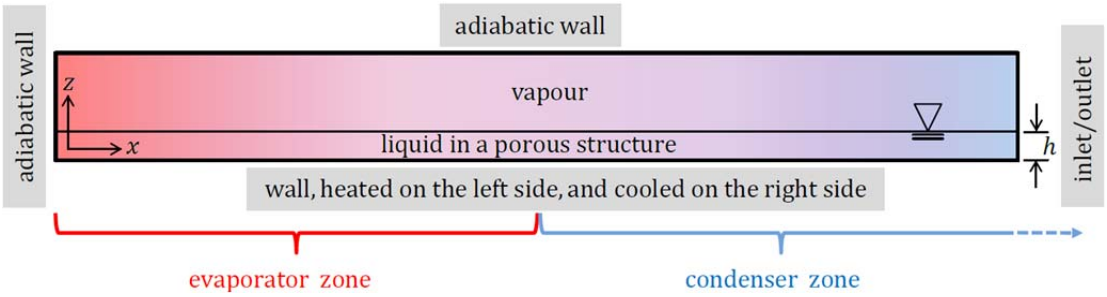

Figure 1: Sketch of the ZGD apparatus in two-dimensional approximation (150 mm x 18.3 mm).

It is assumed that capillary forces within the porous medium are strong enough to compensate the movement caused by evaporation and condensation. As a result, the phase interface can be considered as remaining identical to the solid-vapour boundary shown in Figure 1. Further, it is assumed that the reservoir, which is connected to the apparatus, is isothermal and well-mixed. As a consequence, zero-flux boundary conditions apply for heat and species transfer at the inlet/outlet to the reservoir.
An indicator function α_l that describes the local aggregated liquid and solid volume fraction is defined. This function is similar to that introduced by Hirt and Nichols (1981) for the *Volume-of-Fluid*-(VOF)-method. The initial condition for α_l can be inferred from Figure 1, and α_l remains unchanged during the process. Based on α_l, a *one-field formulated* arbitrary variable Ω is defined as

$$\Omega = \Omega_l \alpha_l + \Omega_v (1 - \alpha_l) \tag{1}$$

with Ω_l *and* Ω_v denoting Ω within the liquid and vapour phase, correspondingly. The metal foam can be characterised by the porosity ϵ, i.e. the solid void fraction. Further, the effective porosity ϵ_{eff} is defined as

$$\epsilon_{eff} = \frac{\epsilon}{\tau} \tag{2}$$

where τ is the metal foam tortuosity. For the description of fluid dynamics of this system, *direct numerical simulation* (DNS) is hardly applicable because of two reasons. First, the structure of the porous medium is stochastic, so that its actual geometry is unknown. Second, it is not possible to resolve the liquid flow within the pores for the whole ZGD apparatus. This is why we apply here the concept of the *hydrodynamic analogy* (HA) (cf. Kenig, 1997). In the HA-based approach, real complex flow is replaced by simplified patterns, such as plug flow or film-like flow. Such simplified flow patterns allow a rigorous description of heat and species transfer to be accomplished. HA-models represent a reasonable alternative to equilibrium or rate-based stage models and have proven to show a good performance for different separation operations (see, e.g., Shilkin et al., 2006; Brinkmann et al, 2014).
We consider both fluids as Newtonian with constant fluid properties. External body forces are neglected. The vapour phase movement is treated here as a slow film-like flow, directed parallel to the phase interface (i.e. in x-direction). The flow is steady and laminar. Consequently, the Navier-Stokes equation applied for the vapour phase reads as follows:

$$\frac{d^2u_v}{dz^2} = \frac{1}{\mu}\frac{dp_v}{dx} \tag{3}$$

where u_v is the vapour flow velocity, p is pressure, and μ is viscosity. In contrast, the liquid phase movement is modelled as plug flow. It is important to capture the porous medium resistance to the liquid-phase flow. This can be done by using Darcy's law (see Nield and Bejan, 1999):

$$-u_l = \frac{K}{\mu}\frac{dp_l}{dx} \tag{4}$$

Here, u_l denotes the volumetrically averaged liquid flow velocity, which has to be distinguished from the flow velocity within the pores defined as $u_{l,P} = u_l/\epsilon$. The permeability K is an empirical parameter depending on the porous structure. From the analysis of the literature, the value $K = 10^{-11}m^2$ can be taken for high resistances of metal foams (Despois and Mortensen, 2005). Eq(4) can be used to determine the pressure drop along the liquid within the porous structure. The liquid-side total pressure drop has to be balanced by the capillary pressure drop described by the *Young-Laplace* equation

$$\Delta p = \frac{4\sigma\cos(\Theta)}{d} \tag{5}$$

with the surface tension σ, contact angle Θ and effective pore diameter d. Eq(5) is applied to determine a value of d at which the liquid-side and capillary pressure drops are balanced. K and d can then be used to evaluate the suitability of porous structures for ZGD. As boundary conditions for Eqs(3) and (4), we applied the no-slip condition at the top wall and at the phase interphase. Since Eq(4) can describe plug flow only, it is not possible to use the no-slip condition at the bottom wall and shear-stress equality at the phase interface. However, the influence of this obstacle on the heat and species transport is low, due to dominating diffusive phenomena in this small-scale process. This has been confirmed by our preliminary simulation studies.
The approach to the description of coupled transport phenomena and phase change is similar to that published in a recent paper (Rieks and Kenig, 2018). A one-field formulated heat transport equation according to Juric and Tryggvason (1988) and Nield and Bejan (1999) is

$$\frac{\partial(\epsilon\rho c_p T + (1-\epsilon)\rho_s c_{p,s} T)}{\partial t} + \nabla\cdot\left(\rho u c_p T\right) - \nabla\cdot(\lambda\nabla T) - \Lambda\dot{m}\delta + \dot{m}(c_{p,l} - c_{p,v})T\delta = 0 \tag{6}$$

with the specific heat capacity c_p, temperature T, density ρ**,** thermal conductivity λ, specific heat of evaporation Λ, and the interfacial mass flux $\dot{m}$. Further, δ is a numerical Dirac-function, which is zero in the fluid phases and large in cells containing the interface. Thermodynamic equilibrium condition is used as a boundary condition at the phase interface. The effective thermal conductivity $\lambda_{l,eff}$ in the liquid-solid region largely depends on the porous material. Bhattacharya et al. (2002) proposed the following equation, which was experimentally validated for highly porous metal foams:

$$\lambda_{l,eff} = 0.35[\epsilon\lambda_l + (1-\epsilon)\lambda_s] + 0.65[\frac{\epsilon}{\lambda_l} + \frac{1-\epsilon}{\lambda_s}]^{-1} \tag{7}$$

Species transfer is described using a two-field formulated approach based on the work by Fleckenstein and Bothe (2015):

$$\frac{\partial(\alpha_l^* c_l \epsilon)}{\partial t} + \nabla\cdot(\alpha_l^* c_l u_l) - \nabla\cdot(D_{l,eff}\nabla c_l) - \dot{m}_{sp}\delta = 0 \tag{8}$$

$$\frac{\partial(\alpha_v^* c_v)}{\partial t} + \nabla\cdot(\alpha_v^* c_v u_v) - \nabla\cdot(D_v\nabla c_v) + \dot{m}_{sp}\delta = 0 \tag{9}$$

Here, the function α_l^* takes the value one in cells filled with the liquid phase, including cells that are cut by the phase interface. In other cells, α_l^* is zero. The function α_v^* is considered in a similar way for the vapour phase. D_l and D_v the diffusivity of species sp in the liquid and vapour phase, respectively. Thermodynamic equilibrium relationship serves as a boundary condition at the phase interface. The effective diffusivity within the liquid-solid region is determined as follows (cf. Baehr and Stephan, 2013):

$$D_{l,eff} = \epsilon_{eff} D_l \tag{10}$$

All equations were implemented into the OpenFOAM® software. They were solved sequentially and iteratively. The total and species interfacial mass fluxes, $\dot{m}$ and $\dot{m}_{sp}$, were determined using iterative numerical algorithms, which also ensure the thermodynamic equilibrium boundary conditions to be fulfilled at the phase interface. Furthermore, the total mass flow rate $\dot{M}(x)$, which is required for flow velocity determination, was obtained by using $\dot{m}$-values and mass balances of ZGD unit sections for arbitrary x-values.
The simulation code was used to determine steady-state solutions applying a relaxation method. The latter ensures numerical simulation stability. To start simulations, we defined the following initial conditions: The system was isothermal at an average process temperature; the fluids were in thermodynamic equilibrium, and at rest. These initial conditions may influence the numerical solution procedure, but not the steady-state solution itself. In general, the simulation code is not limited by steady-state problems. It can equally well be applied to describe transient processes, e.g., ZGD start-up.

3. Simulation results and discussion

Distillation of a methanol/ethanol mixture at $p = 0.15\ \mathrm{bar}$ was simulated. Fluid properties were taken from Linstrom et al. (2016). Equilibrium data and diffusivities were determined with the methods proposed by Poling et al. (2001). Copper was considered to be the solid material. Tortuosity influence on ϵ_{eff} was neglected, and therefore, the value of τ was set to one. Furthermore, very large porosities were chosen in order to minimise the computational effort. The metal foam parameters are summarised in Table 1.

Table 1: Metal foam parameters for case studies on methanol/ethanol mixture ZGD

	Case 1 (reference)	Case 2	Case 3
Metal foam porosity [%]	99.8	99.5	99.8
Metal foam thickness [mm]	2 mm	2 mm	3 mm

For the solution of the problem considered, a thermal boundary condition at the heated/cooled wall had to be defined. We simulate here only a part of the entire ZGD; therefore, a pre-defined T-profile is used as the bottom-wall boundary condition. This profile is taken from a preliminary measurement of a similar capillary structure (copper structure with triangular-shaped grooves) at the TU Darmstadt.
The simulated temperature, flow velocity and ethanol mass fraction (heavy boiling component) fields for Case 1 are shown in Figure 2. At the bottom of the apparatus, heat is transported through the liquid/solid phase (porous structure filled with liquid), leading to evaporation and condensation (phase changes) at the interface. Accompanied by phase change, vapour phase flows in positive x-direction. Along the x-axis, the vapour flow velocity magnitude has a maximum. Between this point and the vertical wall, evaporation leads to a steady increase in the mean vapour flow velocity. Between this point and the inlet/outlet, vapour begins to condense, lowering the mean vapour flow velocity. The liquid flow velocity shows a similar behaviour, but in opposite (negative) x-direction. The ethanol mass fraction field (w_{eth}) reveals that this heavy boiling component is accumulated at the evaporator side, whereas the accumulation of the light boiling component takes place at the condenser side. We will now use Case 1 as a reference for other considered cases.
Figure 3 shows simulation results for Case 2. Here, a lower porosity was used. The most significant impact of this change is that, due to the high thermal conductivity of copper, $\lambda_{l,eff}$ increases. Thus, a smaller resistance to heat transport is exhibited within the liquid and solid, and, as a consequence, heat transfer is more intense, leading to higher phase change rates. This can be seen in the flow velocity fields of both phases. In the vapour phase, large flow velocities lead to deformation of the isotherms, which can partly be attributed to a higher mean flow velocity, resulting in increased velocity gradients in z-direction (cf. dashed frames in Figures 2 and 3). In the liquid phase at the evaporator, the maximum ethanol weight fraction is increased. This happens, because heat transfer is intensified, and thus, a more significant counter-current flow is established, leading to a better separation effect.
Figure 4 shows the simulation results for Case 3, with a thicker porous copper layer. This leads to an increased heat transfer resistance, resulting in less intense phase change, and hence, lower flow velocities than in the reference case. However, the change in the flow velocities is less significant here than due to porosity variation. As a consequence, the vapour phase temperatures are similar to the reference case, and so are the ethanol mass fractions. Thus, porosity influence on the ZGD process is more significant than porous medium thickness, at least for highly porous copper structures.
For Cases 1-3, d-values determined with Eq(5) were larger than 1 mm. This means that, if the pore diameter of the solid structure is smaller than 1 mm, capillary forces are strong enough to compensate phase-change-related liquid movements. A d-value of 1 mm is reasonable for manufacturing. We can assume that for the

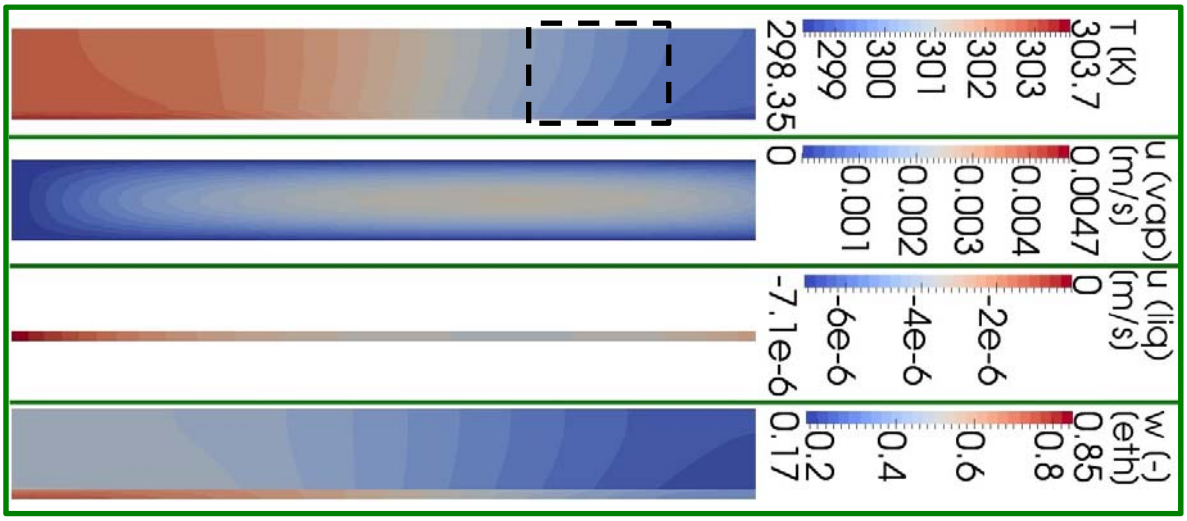

Figure 2: Simulation results for Case 1 (reference): temperature, flow velocity and ethanol mass fraction fields

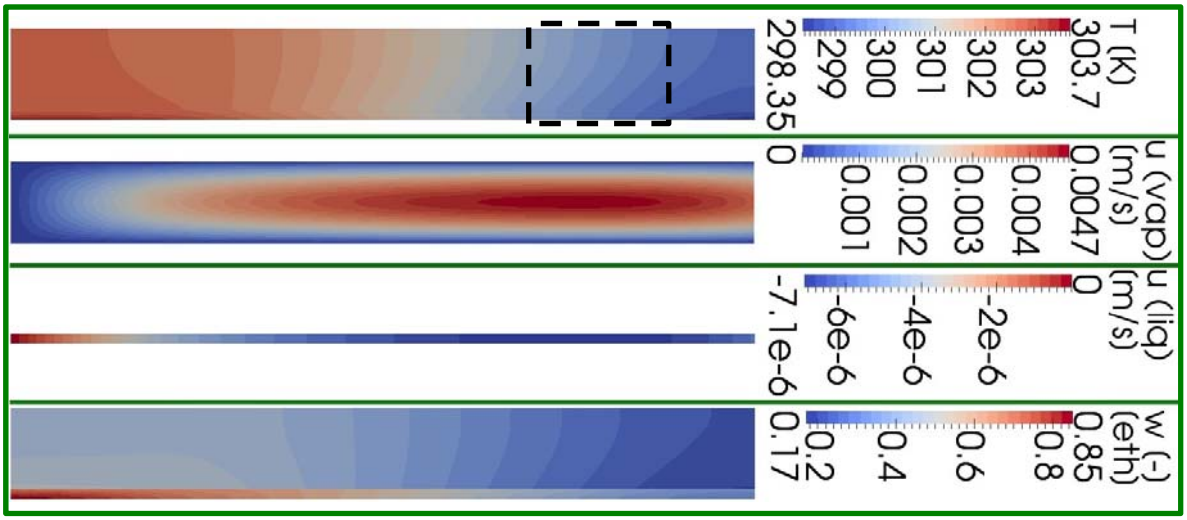

Figure 3: Results for Case 2 (porosity 99.5%); temperature, flow velocity and ethanol mass fraction fields

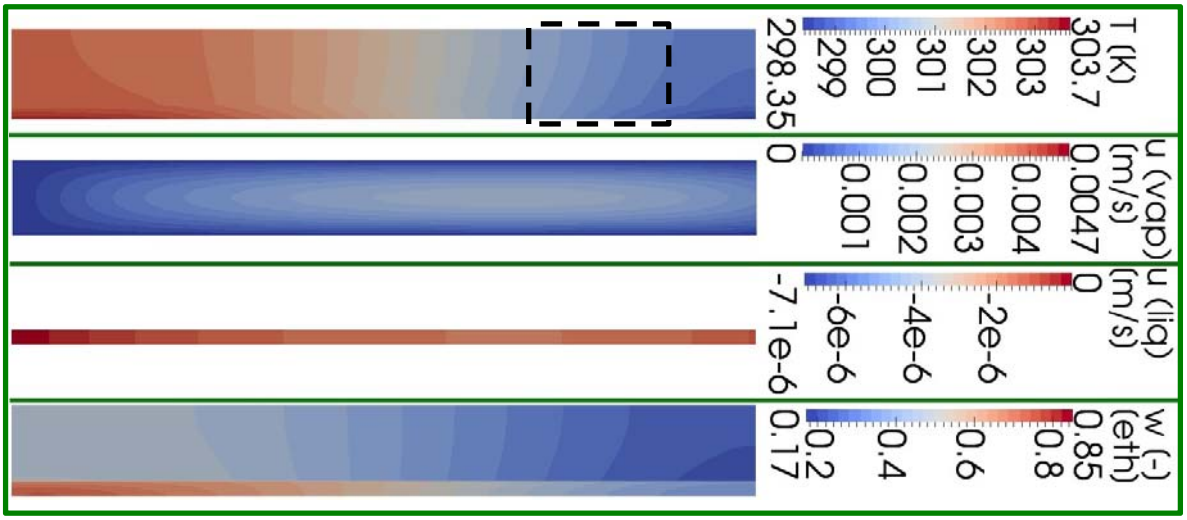

Figure 4: Results for Case 3 (metal foam thickness 3mm); temperature, flow velocity and ethanol mass fraction fields

high porosity values considered in this first study, the simulated ZGD process appears feasible. The height equivalent to a theoretical plate (HETP) was estimated with the established McCabe-Thiele method. The HETP-values determined for Cases 1-3 were around 7 cm. These values show that the simulated separation process is quite efficient compared to conventional distillation units.

4. Conclusions

A new model to capture strongly coupled transport phenomena in ZGD processes was developed. It was used to simulate methanol/ethanol separation processes. The influence of the metal foam porosity and the metal foam thickness were numerically investigated. It could be seen that the metal foam porosity influences the evaporation and condensation rates more significantly than the porous medium thickness. The larger rates of phase change lead to an intensified counter-current flow, which improves the methanol/ethanol separation. This result can help to properly design ZGD units. The simulated ZGD processes can be rated as efficient ($HETP \approx 7\mathrm{cm}$) in comparison to conventional distillation operations. However, the obtained results should be confirmed by further studies, since the bottom temperature profile used as a boundary condition was rather a first approximation. Furthermore, so far, only very high porosities were considered.
As the next steps, simulations for lower porosities and an experimental model validation are planned.

Acknowledgments

We are grateful to Deutsche Forschungsgemeinschaft (DFG) for financial support (projects KE 837/23-1 and GA736/7-1).

References

Baehr H.D., Stephan K., 2013, Wärme- und Stoffübertragung. Springer-Verlag, Berlin Heidelberg, Germany, DOI: 10.1007/978-3-642-36558-4

Bhattacharya A., Calmidi V.V., Mahajan R.L., 2002, Thermophysical properties of high porosity metal foams, Int. J. Heat Mass Trans. 45, 1017-1031, DOI: 10.1016/S0017-9310(01)00220-4

Brinkmann, U., Janzen, A., Kenig, E.Y., 2014, Hydrodynamic analogy approach for modelling reactive absorption. Chem. Eng. J. 250, 342-353, DOI: 10.1016/j.cej.2014.03.066

Despois, J.-F., Mortensen, A., 2005, Permeability of open-pore microcellular materials. Acta Materialia 53, 1381-1388, DOI: 10.1016/j.actamat.2004.11.031

Fleckenstein S., Bothe D., 2015, A volume-of-fluid-based numerical method for multi-component mass transfer with local volume changes, J. Comput. Phys. 301, 35-58, DOI: 10.1016/j.jcp.2015.08.011

Hirt C.W., Nichols B.D., 1981, Volume of fluid (VOF) method for the dynamics of free boundaries, J. Comput. Phys. 39, 201-225, DOI: 10.1016/0021-9991(81)90145-5

Juric D., Tryggvason G., 1998, Computations of boiling flows, Int. J. Multiphase Flow. 24, 387-410, DOI: 10.1016/S0301-9322(97)00050-5

Kenig E.Y., 1997, Multicomponent multiphase film-like systems: A modelling approach, Computers chem. Eng. (supplement) 21, 355-360, DOI: 10.1016/S0098-1354(97)87527-8

Kenig E.Y., Su Y., Lautenschleger A., Chasanis P., Grünewald M., 2013, Micro-separation of fluid systems: A state-of-the-art review, Sep. Purif. Technol. 120, 245-264, DOI: 10.1016/j.seppur.2013.09.028

Linstrom P.J., Mallard W.G., 2016, NIST Chemistry WebBook, NIST Standard Reference Database Number 69. National Institute of Standards and Technology, Gaithersburg MD, 20899, DOI: 10.18434/T4D303

Nield D.A., Bejan A., 1999, Convection in porous media, Springer, New York, USA, DOI: 10.1007/978-1-4614-5541-7

Poling B.E., Prausnitz J.M., O'Connell J., 2001, The properties of gases and liquids, McGraw-Hill, New York, USA

Ramirez-Gonzalez E.A., Martinez C., Alvarez J., 1992, Modeling zero-gravity distillation, Ind. Eng. Chem. Res. 31, 901-908, DOI: 10.1021/ie00003a036

Rieks S., Kenig E.Y., 2018, Modelling and numerical simulation of coupled transport phenomena with phase change: layer evaporation of a binary mixture, Chem. Eng. Sci. 176, 367-376, DOI: 10.1016/j.ces.2017.10.040

Seok D.R., Hwang S.-T., 1985, Zero-gravity distillation utilizing the heat pipe principle (micro-distillation), AIChE J. 31, 2059-2065, DOI: 10.1002/320 aic.690311215

Shilkin, A., Kenig, E.Y., Olujić, Ž., 2006, A Hydrodynamic-analogy-based model for efficiency of structured packing distillation columns, AIChE J. 52, 3055-3066, DOI: 10.1002/aic.10937

Tschernjaew J., Kenig E.Y., Górak A., 1996, Mikrodestillation von Mehrkomponentensystemen, Chem. Eng. Tech. 68, 272-276, DOI: 10.1002/cite.330680309